Multitracer Studies During Gene Therapy of Hepatoma Cells with Herpes Simplex Virus Thymidine Kinase and Ganciclovir

Uwe Haberkorn, Annette Altmann, Iris Morr, Christine Germann, Franz Oberdorfer and Gerhard van Kaick
Department of Oncological Diagnostics and Therapy, German Cancer Research Center, Heidelberg, Germany

Using different tracers of tumor metabolism, the application of PET for monitoring gene therapy with the suicide gene herpes simplex virus thymidine kinase (HSVtk) is investigated in this in vitro study. **Methods:** Morris hepatoma cells were transfected with a retroviral vector bearing the HSVtk gene, and different clones were established by selection with the neomycin analog G418. Thereafter, uptake measurements using fluorodeoxyglucose (FDG), 3-O-methylglucose, aminoisobutyric acid and methionine were performed in a thymidine kinase (TK)-expressing cell line and in control cells bearing the empty vector in the presence of different concentrations of ganciclovir (GCV). These experiments were done up to 48 hr after the onset of therapy. The values were expressed as Bq/well or as Bq/10^5 cells. **Results:** During GCV treatment therapy, a decrease of the uptake/well was measured for all tracers in the TK-expressing cell line. After normalization to the viable cell number, the uptake for FDG and 3-O-methylglucose increases up to 195% after 24 hr incubation with GCV. A high-pressure liquid chromatography analysis revealed a decline of the FDG-6-phosphate fraction after 48 hr incubation with GCV. Consequently, a normalization of FDG uptake was observed after this incubation period, whereas the 3-O-methylglucose uptake was still increased. Experiments performed with different amounts of TK-expressing cells and control cells showed that these effects are dependent on the percentage of TK-expressing cells. The aminoisobutyric acid uptake decreases to 47%, while the methionine uptake decreases in the acid-insoluble fraction (to 17%) and increases in the acid-soluble fraction (to 150%). **Conclusion:** These data indicate that combinations of the PET tracers used in these experiments may be applied for monitoring gene therapy with HSVtk. The increase in FDG and 3-O-methylglucose uptake in vitro is interpreted as stress reaction of the tumor cells. However, an uncoupling of transport and phosphorylation was observed after 48 hr incubation. The amino acid uptake experiments point to an inhibition of protein synthesis as well as of the neutral amino acid transport.

Key Words: gene therapy; herpes simplex virus thymidine kinase; PET; glucose metabolism

Transfer of the gene encoding the herpes simplex virus thymidine kinase (HSVtk) into tumor cells confers sensitivity towards antiviral agents as acyclovir and ganciclovir (GCV) to these cells. HSVtk phosphorylates GCV to GCV monophosphate, which subsequently is metabolized by host kinases to the triphosphate metabolite and incorporated into the tumor cell DNA leading to DNA chain termination during replication (1,2). This approach has been shown to be effective in the treatment of experimental gliomas (3–5), hepatomas (6) and melanomas (7).

Gene therapy using suicide genes is performed in two steps: first, the tumor is infected with recombinant viruses to introduce the suicide enzyme into the cells. To obtain a sufficient level of enzyme activity in the tumor, multiple infections may be necessary. Second, the nontoxic prodrug is applicated systemically. For the planning and the individualization of gene therapy, the enzyme activity induced in the tumor has to be estimated in order to achieve a therapeutically sufficient enzyme level before the application of the prodrug (8). Moreover, the measurement of therapy effects on the tumor metabolism may be useful for the prediction of therapy outcome at an early stage of the treatment. PET, using tracers of tumor metabolism, has been applied for the evaluation of treatment response in a variety of tumors and therapeutic regimens (9–15), indicating that these tracers deliver useful parameters for the early assessment of therapeutic efficacy.

MATERIALS AND METHODS

Rat hepatoma cells (MH3924A) were used for all experiments. The cells were maintained in culture flasks in RPMI 1640 medium (GIBCO/BRL, Eggenstein, Germany) supplemented with 292 mg/liter glutamine, 100,000 IE/liter penicillin, 100 mg/liter streptomycin and 20% fetal calf serum at 37°C, in an atmosphere of 95% air and 5% CO_2.

Cloning and Selection of Cell Lines

The generation of thymidine kinase (TK)-expressing cell lines was done as described (16). Two cell lines LXSN6 (control line with the empty vector) and LXSNtk8 (a GCV sensitive line with the HSVtk gene) were selected for further studies. Each of the following experiments was done in triplicate. The cells were trypsinized, and 8 × 10^4 cells were seeded in 6-well plates. Two days later, the cells were treated with 0.5 μM, 5 μM and 25 μM GCV. All uptake experiments were performed after 4 hr, 24 hr and 48 hr incubation in the GCV-containing medium.

Fluorodeoxyglucose Uptake

The FDG uptake experiments were performed in glucose-free RPMI 1640 medium supplemented with glutamine and penicillin/streptomycin as described (17). After 30 min preincubation, 37 kBq/ml medium 2-fluoro-2-deoxy-D-(^{14}C)glucose (FDG; Amersham, Braunschweig, Germany; specific activity 10.8 GBq/mmol; radioactive concentration 37 MBq/ml, radiochemical purity 99.5%) and cold FDG in a final concentration of 0.1 mM were added, and the cells were incubated for 10 min. After this incubation period, the medium was removed and the cells were washed twice with ice-cold phosphate buffered saline (PBS). The lysis was done on ice using ice-cold 0.6 M perchloric acid and a cell scraper. Thereafter, the lysates were neutralized with 1 M KOH and 0.5 M Tris/HCl (pH 7).

For scintillation counting, 300 μl of the lysates were mixed with 10 ml of Pico-Fluor-15 (Canberra Packard, Meriden, CT) and counted using a scintillation counter (LSC TRICARB 2500TR, Canberra Packard). The measured radioactivity was standardized to the viable cell number as determined by a Coulter counter (Coulter

Electronics, Dunstable, Bedfordshire, United Kingdom) and the trypan blue method (more than 94% viable cells).

The neutralized samples were then analyzed using high performance liquid chromatography (HPLC) as described (18). Briefly, the radioactivity and the differential refractive index were continuously detected, and the radioactive peak areas were integrated after. For the chromatographic analysis a Waters 600 Multisolvent Delivery System with manual injection (U6K injector) and a Waters 410 differential refractometer at 35°C were used (19). Radioactivity was detected using a Canberra A250 detection system with a liquid scintillation flow cell. The column used was a Eurokat H+ (Eurochrom Knauer GmbH, 300 × 8 mm) with water at 0.7 ml/min as the eluent. The retention time for the FDG-6-phosphate was 7.8 min, whereas FDG eluted at about 9.5 min on the present setup.

3-O-Methylglucose Uptake

After 30 min preincubation, 185 kBq/ml medium 3-O-methyl-D-(^{3}H)glucose (Amersham; specific activity 92.5 GBq/mmol; radioactive concentration 37 MBq/ml, radiochemical purity 99.5%) and cold 3-O-methylglucose in a final concentration of 0.05 mM were added, and the cells were incubated for 10 min. After this incubation period, the medium was removed and the cells were washed twice with ice-cold PBS. The lysis was done on ice using 0.3 M NaOH/10% SDS and a cell scraper.

Bystander Experiments

Cells (8 × 10^4) were seeded in 6-well plates as mixtures of LXSN6 and LXSNtk8 cells with varying amounts of LXSNtk8 cells: 100%, 80%, 40%, 20%, 5% and 0% tk8 cells. Two days later, the cells were incubated for 24 and 48 hr without or with 5 μM GCV. Thereafter, an FDG uptake experiment was performed as described.

Aminoisobutyric Acid (AIB) Uptake

The cells were washed three times with PBS and incubated at 37°C for 15 min in Earle's balanced salt solution. Thereafter, 74 kBq α-[1-^{14}C]AIB (NEN/Dupont; specific activity 1.9 GBq/mmol; radioactive concentration 3.7 MBq/ml, radiochemical purity 98.5%) was added. After 10 min incubation, the cells were washed three times on ice and lysed with ice-cold perchloric acid (0.6 M). The lysate was neutralized with 0.5 M Tris buffer (pH 7) and counted by scintillation counting.

Methionine Uptake

The cells were pulsed with 74 kBq L-[methyl-^{14}C]methionine (Amersham; specific activity 2.07 GBq/mmol; radioactive concentration 37 MBq/ml; radiochemical purity 99%) in RPMI 1640 medium (l-methionine concentration 0.1 mM) for 1 hr in 1 ml medium. After removal of the medium, the cells were washed three times with ice-cold PBS. The lysis was performed with 0.5 M perchloric acid and a cell scraper. After 30 min on ice, the lysate was vortexed and rotated at 1500 × g for 5 min at 0°C. The supernatant was removed, the pellets were washed with 0.5 M perchloric acid and rotated again for 5 min at 0°C. The pellet was resuspended in 1 M NaOH at 37°C. For scintillation counting, 300 μl of the acid-soluble fraction (=supernatant) and the acid-insoluble fraction (=pellet) were mixed with 10 ml of Pico-Fluor-15 and counted by scintillation counting.

RESULTS

The effects of different concentrations of GCV on the viable cell number and the tracer uptake/well are shown in Figure 1. Compared to the control cell line a dose-dependent growth inhibition and also a dose-dependent decrease in tracer uptake/well was observed in the TK-expressing cell line.

After normalization to the viable cell number, the FDG uptake in TK-expressing cells is increased, but no changes are seen with control cells (Fig. 2). The FDG accumulation in TK-expressing cells reaches its maximum after 24 hr exposure followed by a decline near to the control values after 48 hr incubation. An HPLC analysis revealed that most of the radioactivity is phosphorylated after 24 hr exposure to GCV, whereas a dose-dependent decline in the phosphorylated fraction was observed after 48 hr incubation with lower concentrations of GCV, which reached a plateau at 5 μM (Fig. 2C). The 3-O-methylglucose uptake/10^5 cells also increases up to 195% in TK-expressing cells after exposure to GCV (Fig. 3). In contrast to the FDG uptake experiment, no decline of 3-O-methylglucose uptake occurred after 48 hr in the TK-expressing cells.

In bystander experiments, a decrease of the viable cell number and FDG uptake/well with increasing amounts of TK-expressing cells was demonstrated (Fig. 4A). Normalization of the FDG uptake to the viable cell number revealed an increased uptake after 24 hr exposure to 5 μM GCV, which was related to the amount of TK-expressing cells (Fig. 4B). After 48 hr incubation the FDG uptake increases with a maximum for 40% TK-expressing cells and then declines again for 80% and 100% TK-expressing cells (Fig. 4C). The HPLC analysis revealed a decrease in the content of FDG-6-phosphate with an increasing percentage of TK-expressing cells (Fig. 4D).

After exposure to GCV the AIB uptake/10^5 cells decreases in a dose-dependent manner to 47% in the TK-expressing cells, whereas no significant differences between treated and untreated cells are observed in the control cell line (Fig. 5A, B). In the methionine uptake experiments an increase of tracer accumulation during the 48 hr incubation period could be noticed in the untreated cells of both cell lines and also in the treated cells of the control cell line (Fig. 6). After exposure to GCV the methionine uptake decreases in the acid-insoluble fraction (to 17% of the control, Fig. 6A, B) and increases in the acid-soluble fraction (to 150% of the control, Fig. 6C, D) of the TK-expressing cell line. The overall effect of gene therapy with HSVtk and GCV on the uptake of the different tracer is summarized in Table 1.

DISCUSSION

After exposure of a TK-expressing Morris hepatoma cell line to GCV, a dose-dependent decline of the uptake/well [which can be considered as a simple model of tumor uptake (20)] of all tracers used was noticed (Fig. 1). The uptake of AIB and methionine decreases earlier (after 24 hr) than that of the glucose tracers (after 48 hr). These data seem to be at variance with data of Higashi et al. (20), who found no decrease of the methionine and FDG uptake/well early after irradiation of an ovary human adenocarcinoma cell line. This discrepancy might be explained by the different cell lines as well as by the different therapies used in both studies.

Standardization to the viable cell number revealed an enhancement of both FDG and 3-O-methylglucose uptake after a 24 hr incubation period with GCV (Figs. 2 and 3). After 48 hr, the FDG uptake declines near to the control values. This increased uptake of the glucose transport tracer 3-O-methylglucose over the whole incubation period together with the normalization of the FDG accumulation may be caused by a loss in the phosphorylating capacity of hexokinase, which leads to a relative increase of the FDG/FDG-6-phosphate ratio. In contrast to FDG-6-phosphate, which is trapped due to its negative charge, FDG can be transported out of the cell. Consequently, less phosphorylation of FDG by the hexokinase
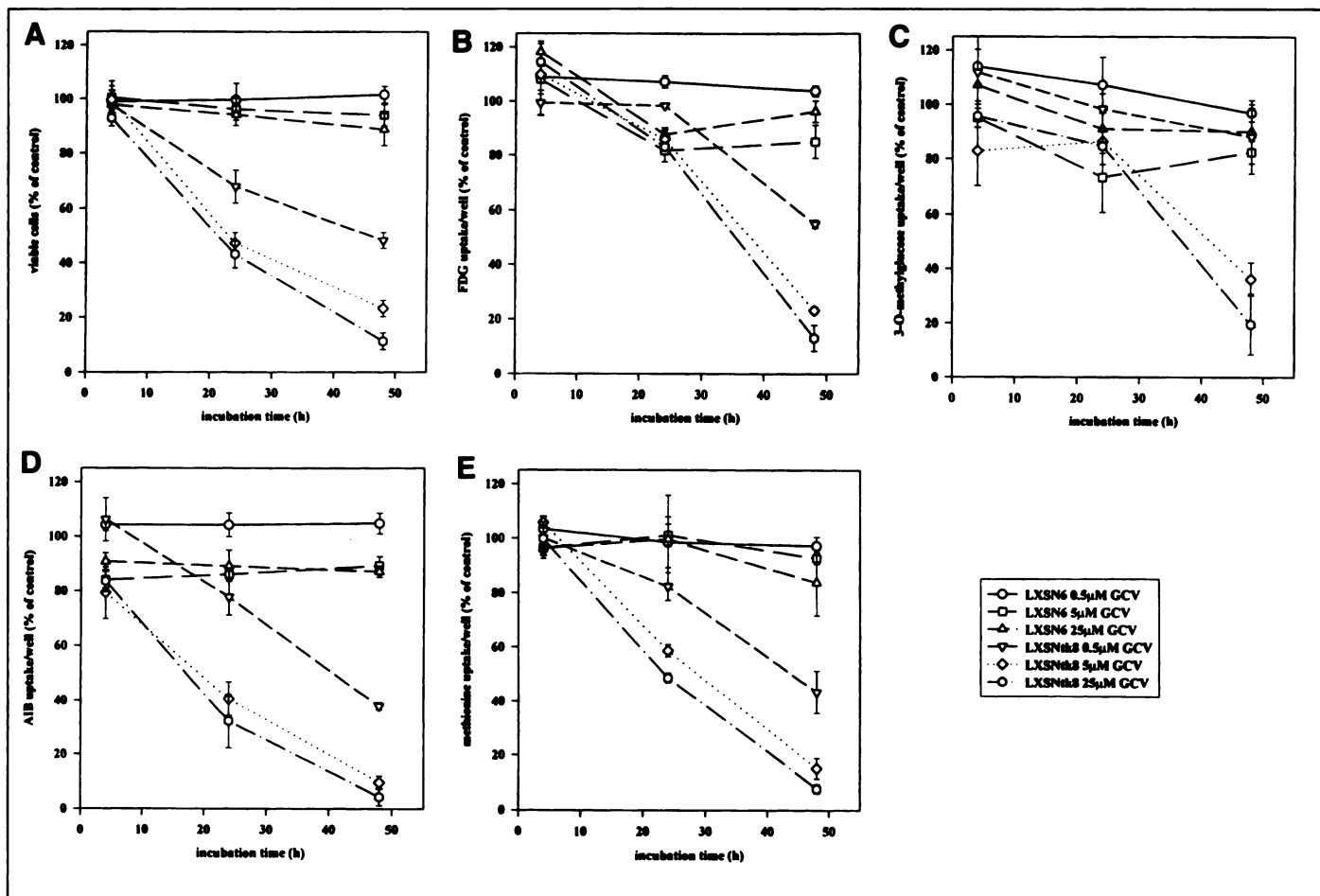
FIGURE 1. Growth inhibition (A) and tracer uptake/well for FDG (B), 3-O-methylglucose (C), AIB (D) and methionine (E) in TK-expressing cells (LXSNtk8) and in control cells (LXSN6) after different incubation periods with 0.5, 5 and 25 μM GCV. Mean and s.d. (n = 3).

may result in decreased FDG trapping. In a HPLC analysis of the cell lysates, we observed a decrease of the FDG-6-phosphate content after 48 hr incubation with GCV (Fig. 2C). Consequently, the FDG content rises relative to the FDG-6-phosphate fraction. An increase in dephosphorylation, which may be another reason for a relative enhancement of the FDG content seems unlikely, since the dephosphatase expression is down-regulated during the malignant transformation.

Two observations point to the therapeutic effect of the HSVtk/GCV system as the cause of this uncoupling of glucose transport and phosphorylation: (a) the decrease in FDG-6-phosphate after 48 hr incubation is a function of the GCV dose at least for lower concentrations, and (b) the results of the bystander experiments showed that the phenomenon of decreasing FDG-6-phosphate content is a function of the percentage of TK-expressing cells and, therefore, a function of TK activity (Fig. 4D). The competition of HSVtk and hexokinase for the ATP pool in the cell may cause a decrease in the phosphorylated FDG metabolite. In addition, a depletion of the ATP pool due to an extensive activity of HSVtk may occur. Alternatively,
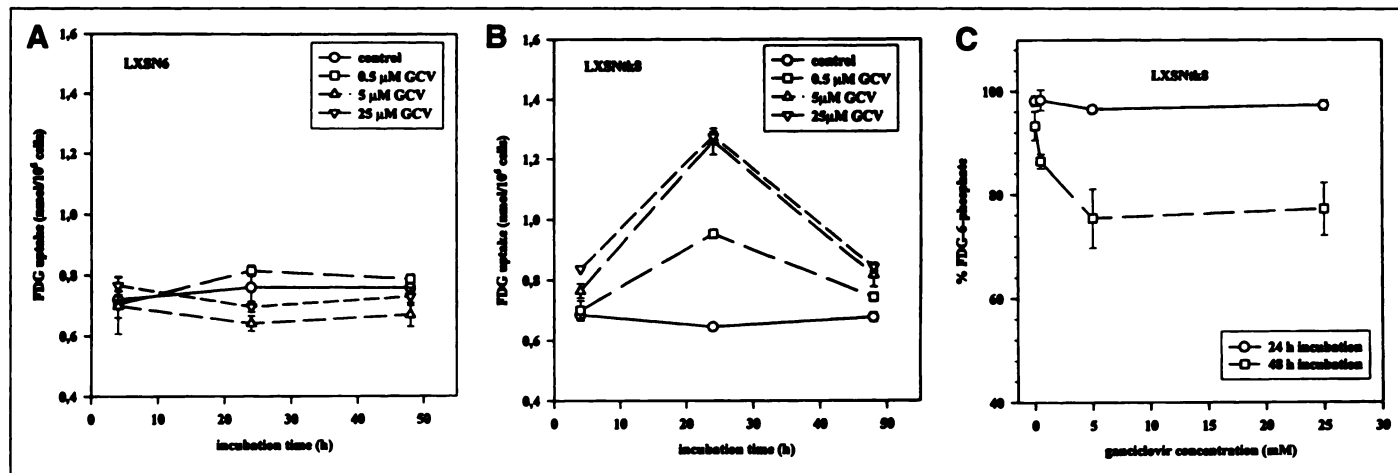

FIGURE 2. FDG uptake (nmol/10^5 cells) in control cells (A) and TK-expressing cells (B) after different incubation periods with 0.5, 5 and 25 μM GCV. Content of FDG-6-phosphate (C) after 24 and 48 hr exposure to the indicated concentrations of GCV. Mean and s.d. (n = 3).
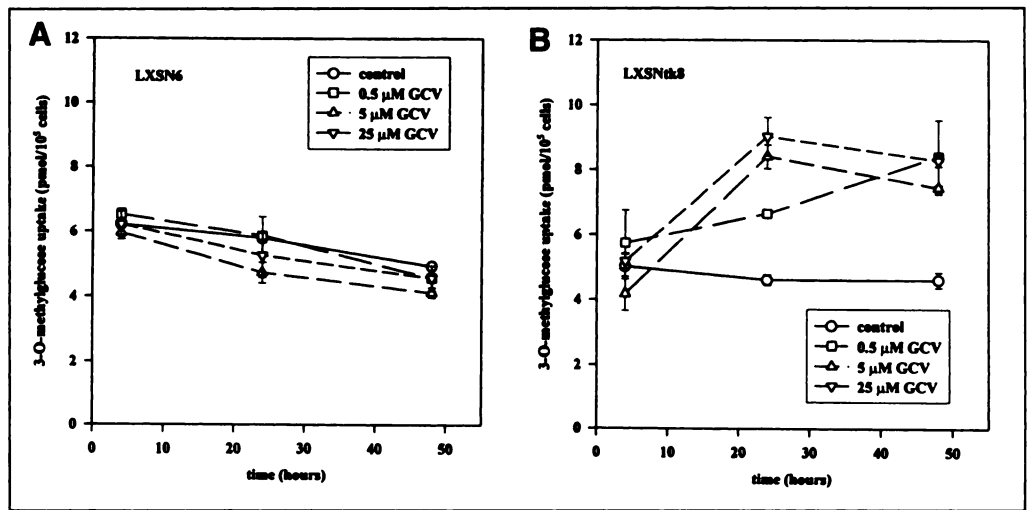
FIGURE 3. 3-O-Methylglucose uptake (pmol/10⁵ cells) in control cells (A) and TK-expressing cells (B) after different incubation periods with 0.5, 5 and 25 μM GCV. Mean and s.d. (n = 3).

the observed phenomenon may be produced by a therapy-induced inhibition of the synthesis of hexokinase. Evidence for this explanation may be derived from the decreased methionine incorporation in the acid-insoluble fraction (Fig. 6B), indicating an impaired protein synthesis.

In clinical and experimental studies, an increase of FDG uptake early after treatment of malignant tumors was observed (11,17,18,21–23). Comparable experiments with rat adenocarcinoma cells under chemotherapy revealed that this effect is predominantly caused by an enhanced glucose transport (17). As underlying mechanism, a redistribution of the glucose

transport protein from intracellular pools to the plasma membrane, may be considered and is observed in cell culture studies as a general reaction to cellular stress (24–27). Since prodrug activation by the HSVtk leads to DNA chain termination and cell damage, the same reactions may also occur in tumor cells under gene therapy with this suicide system. Translocation of glucose transport proteins to the plasma membrane as a first reaction to cellular stress may cause enhancement of glucose transport and represents a short-term regulatory mechanism that acts independent of protein synthesis.

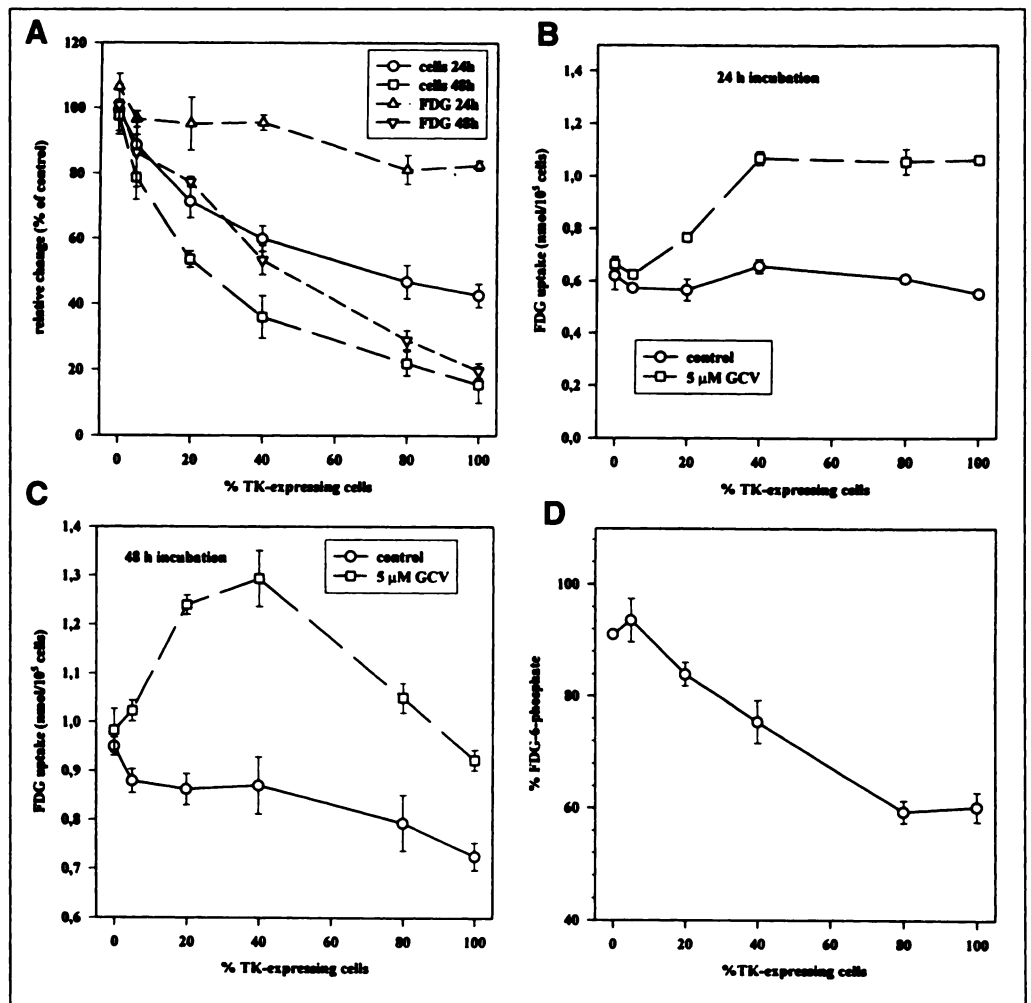To ensure a complete tumor regression, TK expression in

FIGURE 4. Growth inhibition, FDG uptake/well (A) and FDG uptake/10⁵ cells (B,C) in mixtures of TK-expressing cells and control cells after 24 and 48 hr incubation with 5 μM GCV. Content of FDG-6-phosphate (D) after 48 hr exposure to GCV. Mean and s.d. (n = 3).
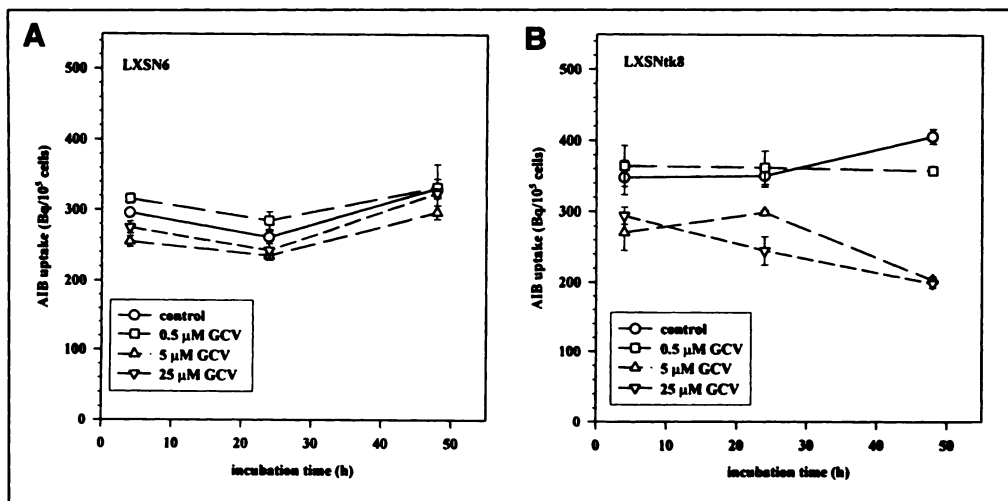
FIGURE 5. AIB uptake (Bq/10⁵ cells) in control cells (A) and TK-expressing cells (B) after different incubation periods with 0.5, 5 and 25 μM GCV. Mean and s.d. (n = 3).

every individual tumor cell is not necessary (*3,4*). Tumor cells that are not infected with the viral vector encoding the suicide gene and are located in the neighborhood of TK-expressing cells become sensitive to GCV ("bystander effect"). Studies performed to investigate the bystander effect revealed that the decrease in viable cell number depends on the percentage of TK-expressing cells. Similar results were obtained when the FDG uptake/well was measured after a 48 hr incubation period with GCV (Fig. 4A). In contrast, incubation of the cells for 24 hr with the prodrug does not lead to a decrease of the FDG uptake/well, despite a decline of the viable cell number. This is caused by an increase of the FDG uptake in the remaining

tumor cells (Fig. 4B), which compensates for the loss in glucose-consuming cells. The fact that after longer incubation periods (48 hr) an uncoupling of the glucose transport and phosphorylation. occurs as a function of the percentage of TK-expressing cells (Figs. 2, 3, 4 C, D) indicates that in vivo measurements with double tracer techniques (FDG and 3-O-methylglucose) and/or compartment analysis may be superior to the determination of standardized uptake values. Recently, Hariharan et al. compared rates of cardiac glucose utilization with the FDG uptake before and after changes in the physiological environment of the heart (*28*). The uptake and retention of FDG in heart muscle was linearly related to the glucose
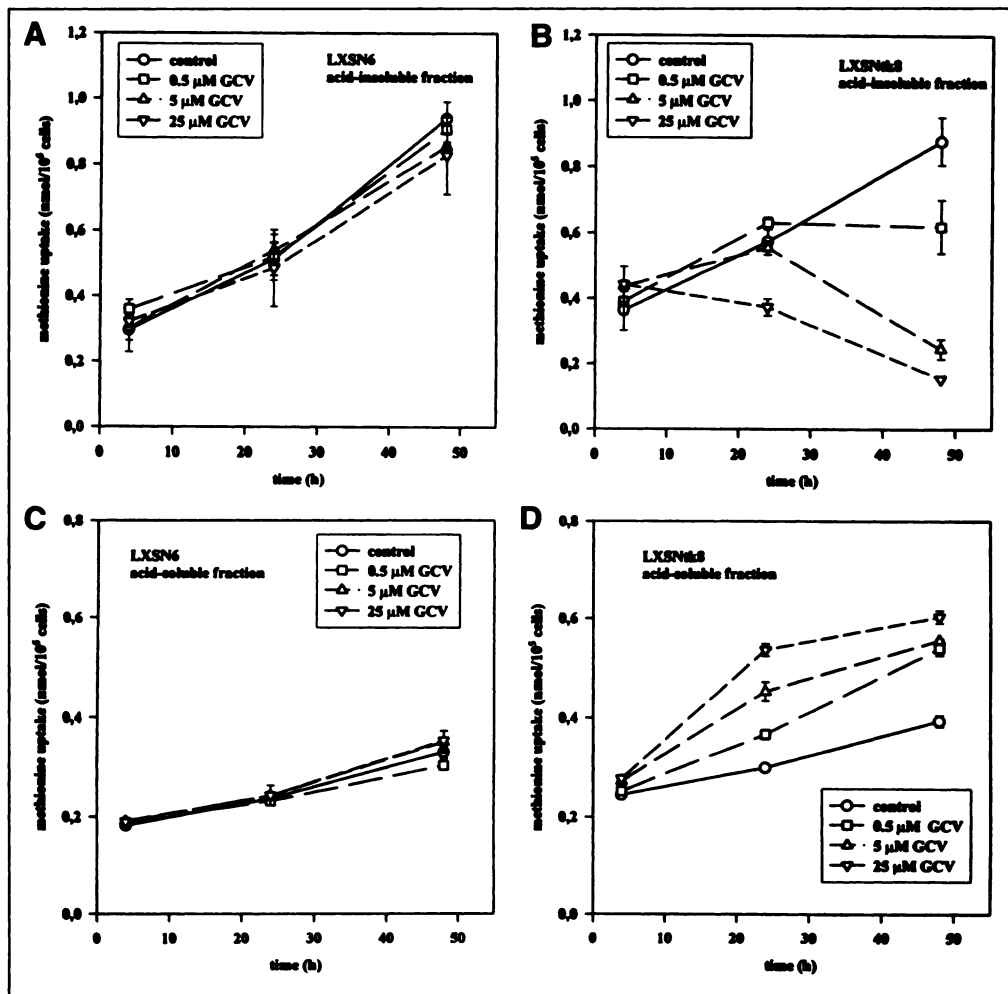

FIGURE 6. Methionine uptake (nmol/10⁵ cells) in the acid-insoluble (A,B) and the acid-soluble (C,D) fraction in control cells (A,C) and TK-expressing cells (B,D) after different incubation periods with 0.5, 5 and 25 μM GCV. Mean and s.d. (n = 3).

TABLE 1

Changes of FDG, 3-O-Methylglucose, AIB and Methionine in TK-Expressing Cells After 4-, 24- and 48-Hour Incubation with GCV

Tracer	4 hr	24 hr	48 hr
FDG	±	↑	(↑)
3-O-Methylglucose	±	↑	↑
AIB	±	↓	↓
Met (soluble)	±	↑	↑
Met (insoluble)	±	↓	↓

± = no change; ↓ = decrease; ↑ = increase; (↑) = moderate increase; Met = methionine.

utilization only under steady-state conditions. However, the FDG uptake underestimated the glucose metabolism under nonphysiological stress, thereby precluding the determination of absolute rates of myocardial glucose uptake by the FDG uptake under nonsteady-state conditions. This again underlines the necessity of using either a double-tracer technique or a compartment analysis for the assessment of therapy-induced changes in glucose metabolism.

Studies including different human tumors that have been treated by a variety of therapies and animal experiments in the rat AH109A tumor model after radiotherapy demonstrated a rapid post-therapeutic reduction of [^{14}C]methionine uptake, reflecting an inactivation of protein synthesis and also a damage of the membrane transport system (13–15,29). Moreover, the accumulation of AIB, a synthetic amino acid, which was shown to be taken up mainly by the A type transport system (30,31), is decreased in rat prostate tumors after long-term treatment with stilbestrol (32). In vitro studies demonstrated that methotrexate and cisplatin induce a decline of AIB and methionine accumulation in L1210 murine leukemia cells (33,34). The authors speculated that the inhibition of methionine uptake by methotrexate may be due to drug binding to a specific membrane carrier or reduction of the sodium gradient across the plasma membrane necessary for the uptake of amino acids or effects on intracellular processes that support uptake of amino acids (34). Higashi et al. demonstrated an increase of the methionine and FDG uptake in human ovarian carcinoma cells after radiotherapy accompanied by an enlargement of the cell volume (20). These phenomena were interpreted as giant cell formation with continued protein synthesis, but an accelerated repair was also discussed (20). This study combined the information obtained by experiments using a transport tracer (AIB) and a tracer that is transported and metabolized (methionine). We found a decrease of neutral amino acid transport after therapy (Fig. 5). Furthermore, the decrease of the radioactivity in the acid-insoluble fraction (representing nucleic acids and proteins) in the methionine experiment indicates that the protein synthesis is also impaired (Fig. 6). The increase of the radioactivity in the acid-soluble fraction may be caused by enhanced transmethylation processes, which are usually observed during oncogenic transformation and after exposure to DNA-damaging agents (35).

We observed an increase in methionine uptake during the 48 hr incubation period in untreated TK-expressing cells and also in the control cell line (treated and untreated). Variations in uptake of thymidine and methionine between different phases of the cells have been described by Higashi et al. in human adenocarcinoma cells (36). Therefore, these variations of methionine uptake during the cell cycle may be an explanation for this phenomenon.

In conclusion, we performed uptake studies with combina-

tions of a transport tracer (AIB, 3-O-methylglucose) and a tracer for transport and metabolism (methionine, FDG) in cells during gene therapy with the HSVtk/GCV suicide system. Whereas the AIB and methionine uptake produce identical effects on transport and protein synthesis, the results obtained with 3-O-methylglucose and FDG reveal an uncoupling of transport and phosphorylation with increased glucose transport (Table 1). These data indicate that these tracer combinations may also be useful in vivo for the exact evaluation of metabolic reactions after tumor therapy.

REFERENCES

1. Keller PM, Fyfe JA, Beauchamp L, et al. Enzymatic phosphorylation of acyclic nucleoside analogs and correlations with antiherpetic activities. Biochem Pharmacol 1981;30:3071–3077.
2. Moolten FL. Tumor chemosensitivity conferred by inserted herpes thymidine kinase genes: paradigm for a prospective cancer control strategy. Cancer Res 1986;46:5276–5281.
3. Culver KW, Ram Z, Walbridge S, et al. In vivo gene transfer with retroviral vector-producer cells for treatment of experimental brain tumors. Science 1992;256:1550–1552.
4. Ram Z, Culver WK, Walbridge S, et al. In situ retroviral-mediated gene transfer for the treatment of brain tumors in rats. Cancer Res 1993;53:83–88.
5. Takamiya Y, Short MP, Ezzedine ZD, Moolten FL, Breakfield XO, Martuzza RL. Gene therapy of malignant brain tumors: a rat glioma line bearing the herpes simplex virus type 1-thymidine kinase gene and wild type retrovirus kills other tumor cells. J Neurosci Res 1992;33:493–503.
6. Huber BE, Richards CA, Krenitsky TA. Retroviral-mediated gene therapy for the treatment of hepatocellular carcinoma: an innovative approach for cancer therapy. Proc Natl Acad Sci USA 1991;88:8039–8043.
7. Vile RG, Hart IR. Use of tissue-specific expression of the herpes simplex virus thymidine kinase gene to inhibit growth of established murine melanomas following direct intratumoral injection of DNA. Cancer Res 1993;53:3860–3864.
8. Haberkorn U, Oberdorfer F, Gebert J, et al. Monitoring of gene therapy with cytosine deaminase: in vitro studies using ^{3}H-5-fluorocytosine. J Nucl Med 1996;37:87–94.
9. Wahl RL, Cody RL, Hutchins CD, Mudgett EE. Primary and metastatic breast carcinoma: initial evaluation with PET with the radiolabeled glucose analog 2-(F-18)-fluoro-2-deoxy-D-glucose. Radiology 1991;179:765–770.
10. Haberkorn U, Strauss LG, Dimitrakopoulou A, et al. Fluorodeoxyglucose imaging of advanced head and neck cancer after chemotherapy. J Nucl Med 1993;34:12–17.
11. Rozenthal JM, Levine RL, Nickles RJ, Dobkin JA. Glucose uptake by gliomas after treatment. Arch Neurol 1989;46:1302–1307.
12. Minn H, Paul R, Ahonen A. Evaluation of treatment response to radiotherapy in head and neck cancer with fluorine-18-fluorodeoxyglucose. J Nucl Med 1988;29:1521–1525.
13. Bergstrom M, Muhr C, Lundberg PO, et al. Rapid decrease in amino acid metabolism in prolactin-secreting pituitary adenomas after bromocriptine treatment: a PET study. J Comput Assist Tomogr 1987;11:815–819.
14. Jansson T, Westlin JE, Ahlstrom H, Lilja A, Langstrom B, Bergh J. Positron emission tomography studies in patients with locally advanced and/or metastatic breast cancer: a method for early therapy evaluation? J Clin Oncol 1995;13:1470–1477.
15. Kubota K, Yamada S, Ishiwata I, et al. Evaluation of the treatment response of lung cancer with positron emission tomography and L-(methyl-^{11}C)methionine: a preliminary study. Eur J Nucl Med 1993;6:495–501.
16. Haberkorn U, Altmann A, Morr I, et al. Gene therapy with herpes simplex virus thymidine kinase in hepatoma cells: uptake of specific substrates. J Nucl Med 1997;38:287–294.
17. Haberkorn U, Morr I, Oberdorfer F, et al. Fluorodeoxyglucose uptake in vitro: aspects of method and effects of treatment with gemcitabine. J Nucl Med 1994;35:1842–1850.
18. Haberkorn U, Reinhardt M, Strauss LG, et al. Metabolic design of combination therapy: use of enhanced fluorodeoxyglucose uptake caused by chemotherapy. J Nucl Med 1992;33:1981–1987.
19. Oberdorfer F, Kemper K, Kaleja M, Reusch J, Gottschall K. Carbohydrate analysis with ion chromatography using eurokat stationary phases: preparative separation of monosaccharides and their fluorinated derivatives. J Chromatogr 1991;552:483–487.
20. Higashi K, Clavo AC, Wahl RL. In vitro assessment of 2-fluoro-2-deoxy-D-glucose, L-methionine and thymidine as agents to monitor the early response of a human adenocarcinoma cell line to radiotherapy. J Nucl Med 1993;34:773–779.
21. Schaider H, Haberkorn U, Berger MR, Oberdorfer F, Morr I, van Kaick G. Application of α-aminoisobutyric acid, L-methionine, thymidine and 2-fluoro-2-deoxy-D-glucose to monitor effects of chemotherapy in a human colon carcinoma cell line. Eur J Nucl Med 1996;23:55–60.
22. Minn H, Kangas L, Kellokumpu-Lehtinen P, et al. Uptake of 2-fluoro-2-deoxy-D-(U-^{14}C)-glucose during chemotherapy in murine Lewis lung tumor. Nucl Med Biol 1992;19:55–63.
23. Slosman DO, Pugin J. Lack of correlation between tritiated deoxyglucose, thallium-201 and technetium-99m-MIBI cell incorporation under various cell stresses. J Nucl Med 1994;35:120–126.
24. Wertheimer E, Sasson S, Cerasi E, Ben-Neriah Y. The ubiquitous glucose transporter GLUT-1 belongs to the glucose-regulated protein family of stress-inducible proteins. Proc Natl Acad Sci USA 1991;88:2525–2529.
25. Widnell CC, Baldwin SA, Davies A, Martin S, Pasternak CA. Cellular stress induces a redistribution of the glucose transporter. FASEB J 1990;4:1634–1637.
26. Pasternak CA, Aiyathurai JEJ, Makinde V, et al. Regulation of glucose uptake by stressed cells. J Cell Physiol 1991;149:324–331.

27. Clancy BM, Czech MP. Hexose transport stimulation and membrane redistribution of glucose transporter isoforms in response to cholera toxin, dibutyryl cyclic AMP and insulin in 3T3 adipocytes. *J Biol Chem* 1990;265:12434–12443.
28. Hariharan R, Bray M, Ganim R, Doenst T, Goodwin GW, Taegtmayer H. Fundamental limitations of (18F)2-deoxy-2-fluoro-D-glucose for assessing myocardial glucose uptake. *Circulation* 1995;91:2435–2444.
29. Kubota K, Ishiwata K, Kubota R, et al. Tracer feasibility for monitoring tumor radiotherapy: a quadruple tracer study with fluorine-18-fluorodeoxyglucose or fluorine-18-fluorodeoxyuridine, L-[methyl-14C]methionine, [6-3H]thymidine and gallium-67. *J Nucl Med* 1991;32:2118–2123.
30. Christensen HN. Role of amino acid transport and countertransport in nutrition and metabolism. *Physiol Rev* 1990;70:43–76.
31. Conti PS, Sordillo EM, Sordillo PP, Schmall B. Tumor localization of alpha-aminoisobutyric acid (AIB) in human melanoma heterotransplants. *Eur J Nucl Med* 1985;10:45–47.

32. Dunzendorfer U, Schmall B, Bigler RE, et al. Synthesis and body distribution of alpha-aminoisobutyric acid-11C in normal and prostate cancer bearing rat after chemotherapy. *Eur J Nucl Med* 1981;6:535–538.
33. Scanlon K, Safirstein RL, Thies H, Gross RB, Waxman S, Guttenplan JB. Inhibition of amino acid transport by cis-diaminedichloroplatinum (II) derivatives L1210 murine leukemia cells. *Cancer Res* 1983;43:4211–4215.
34. Scanlon K, Cashmore AR, Kashani-Sabet M, et al. Inhibition of methionine uptake by methotrexate in mouse leukemia L1210. *Cancer Chemother Pharmacol* 1987;19:21–24.
35. Hoffman RM. Altered methionine metabolism and transmethylation in cancer. *Anticancer Res* 1985;5:1–30.
36. Higashi K, Clavo AC, Wahl RL. Does FDG uptake measure the proliferative activity of human cancer cells? In vitro comparison with DNA flow cytometry and tritiated thymidine uptake. *J Nucl Med* 1993;34:414–418.

Preclinical Studies of Indium-111-Labeled IgM: A Human Monoclonal Antibody for Infection Imaging

Ramaswamy Subramanian, Shankar Vallabhajoshula, Helena Lipszyc, Quing Zhao, James Murray, Samir Shaban, Josef Machac and Michael G. Hanna, Jr.

PerImmune, Inc., Rockville, Maryland; Division of Nuclear Medicine, Department of Radiology, The Mount Sinai Medical Center, New York, New York

Indium-111-labeled plasma proteins, such as albumin, transferrin and IgG, have been proven useful to image infection. We reported previously that 111In-labeled human monoclonal antibody, IgM 16.88 (In-IgM) also would localize at the site of infection. However, the kinetics of blood clearance, distribution and infection uptake have not been investigated. We compared the kinetics of distribution and infection uptake of In-IgM 16.88 with that of In-polyclonal IgG in rats with focal infection. **Methods:** Both IgM 16.88 and polyclonal IgG were labeled with 111In using a bifunctional chelating agent, LiLo. The labeling efficiency was >95%. Focal infection was induced in rats by an intramuscular injection of E. Coli in the right thigh. In-IgM (30–40 μCi) was injected into five groups of rats (five rats/group). The rats were killed at 4, 8, 16, 24 and 36 hr. The percent injected dose (%ID) in blood, infection muscle, control muscle, liver, spleen and kidney were determined. Similar studies were performed with In-IgG. **Results:** The In-IgM activity in blood at 4 hr postinjection was 27% which decreased to 2% by 36 hr. In contrast, the In-IgG blood activity was 40% at 4 hr and 20% at 36 hr. The infection/muscle (I/M) ratios are higher with In-IgM at all time points postinjection compared to that of In-IgG. At 24 hr, the I/M ratio was 22 compared to 9 with In-IgG. At the same time point, the infection/blood (I/B) ratio with In-IgM was 2.7 compared to only 0.8 with that of In-IgG. In-IgM was taken up mostly by the liver compared to diffuse abdominal uptake of IgG. **Conclusion:** These results indicate that In-IgM produces higher lesion to background ratio when compared to In-IgG and, therefore, is potentially useful to image infection in patients.

Key Words: IgM; indium-111; infection imaging; LiLo; 16.88; human monoclonal antibody

J Nucl Med 1997; 38:1054–1059

The most commonly used radiotracers for imaging occult infection in patients are 67Ga-citrate and radiolabeled (111In or 99mTc) leukocytes (1,2). Although these agents have been shown to be efficacious, several new tracers are being evaluated as potential infection imaging agents. Radiolabeled human

polyclonal IgG and liposomes labeled with 111In or 99mTc have shown potential diagnostic use in experimental infection models (2–6). In addition, several radiolabeled chemotactic peptides also are being evaluated as radiotracers for infection imaging studies (7–9). Due to slow blood clearance of labeled IgG, the target/background and target/blood ratios are suboptimal and delayed imaging at 24 and 48 hr are essential for good quality images. On the other hand, the labeled peptides clear very rapidly from circulation, but the absolute uptake at the site of infection is very low. The mechanism(s) of localization of radiolabeled proteins appears to be nonspecific and the localization is due mostly to increased capillary permeability and extravascular leakage (1–4).

We have developed a human monoclonal antibody belonging to IgM class, designated as IgM 16.88 which can be radiolabeled with 111In using the bifunctional chelating agent LiLo, 1,3-bis[N-N(2-aminoethyl)−2-aminoethyl]−2-aminoacetamido]−2-(4-isothiocyanatobenzyl)propane-N,N,N′,N″,N‴,N⁗,N⁗′,N⁗″-octaacetic acid. We have reported previously that this agent has very high in vitro and in vivo stability (10,11). Preliminary immunohistopathological studies have shown that the LiLo-IgM 16.88 conjugate binds almost exclusively to the dead white blood cells (granulocytes and lymphocytes) while binding to live cells (and red blood cells) was minimal. In a preliminary study, we also observed that 111In-labeled LiLo-IgM 16.88 localizes in the site of experimental infection in rats and that the image quality was better than with 111In-labeled polyclonal and monoclonal IgG preparations (12,13). In order to assess the potential diagnostic use of 111In-LiLo-IgM 16.88 as a tracer to image occult infection, we compared the kinetics of distribution and infection uptake of 111In-LiLo-IgM 16.88 with that of 111In-LiLo-polyclonal human IgG preparation in rats and rabbits with focal infection (14). The results presented here clearly demonstrate that the infection/muscle and infection/blood ratios with In-IgM are significantly higher than with In-IgG.